

A functional proteomics approach links the ubiquitin-related modifier Urm1 to a tRNA modification pathway

Christian D. Schlieker¹, Annemarte G. Van der Veen, Jady R. Damon, Eric Spooner, and Hidde L. Ploegh¹

Whitehead Institute for Biomedical Research, 9 Cambridge Center, Cambridge, MA 02142

Edited by Alexander Rich, Massachusetts Institute of Technology, Cambridge, MA, and approved October 6, 2008 (received for review September 4, 2008)

Urm1 is a highly conserved ubiquitin-related modifier of unknown function. A reduction of cellular Urm1 levels causes severe cytokinesis defects in HeLa cells, resulting in the accumulation of enlarged multinucleated cells. To understand the underlying mechanism, we applied a functional proteomics approach and discovered an enzymatic activity that links Urm1 to a tRNA modification pathway. Unlike ubiquitin (Ub) and many Ub-like modifiers, which are commonly conjugated to proteinaceous targets, Urm1 is activated by an unusual mechanism to yield a thiocarboxylate intermediate that serves as sulfur donor in tRNA thiolation reactions. This mechanism is reminiscent of that used by prokaryotic sulfur carriers and thus defines the evolutionary link between ancient Ub progenitors and the eukaryotic Ub/Ub-like modification systems.

cytokinesis | thiolation | urmylation | wobble nucleoside | MOCS3

The covalent attachment of ubiquitin (Ub) and ubiquitin-like modifiers (Ubls) to target molecules serves many different functions: Ub and Ubls have been implicated in processes as diverse as protein degradation, modulation of enzymatic activity, control of subcellular localization, and mobilization of defined subunits from complex assemblies (1). Although the functional outcomes are quite diverse, most if not all Ubls employ a similar activation mechanism before conjugation to their targets. Accordingly, Ub/Ubls exhibit remarkably similar structural properties, a feature that also applies to the enzymes that act on them.

The Ub-like β -grasp fold is the structural hallmark common to all representatives of the Ub family [supporting information (SI) Fig. S1]. In the first of several steps that constitute an enzymatic cascade, Ub/Ubl is activated by an activating enzyme (*E1*) to form an acyl-adenylate at the C terminus. This is followed by thioester formation with the active-site cysteine of the *E1* enzyme, and, eventually, further transesterification events to downstream activities (*E2s* and *E3s*). The latter confer substrate specificity to the process by conjugating the activated Ub/Ubl to its selected target (2, 3). Ub, NEDD8, SUMO-1, and other Ubls are ultimately transferred to the ϵ -amino group of a lysine residue in a proteinaceous target to yield an isopeptide-linked Ub/Ubl conjugate. Atg8 and LC3 are attached to phospholipids, and other classes of molecular targets might exist (for a current review, see ref. 1).

Ub, Ubls, and the corresponding enzymatic cascades appear to be restricted to eukaryotes, although a number of bacterial proteins adopt a Ub-like β -grasp fold (4). ThiS and MoaD are the best-characterized bacterial representatives of this type. Both molecules show little if any sequence identity to Ubls but are structurally similar to Ub (Fig. S1). ThiS and MoaD are activated by adenylation reactions, and the corresponding enzymatic activities, ThiF and MoeB, respectively, are structurally similar to eukaryotic *E1* enzymes (5–7). ThiS and MoaD can thus be considered as molecular ancestors of the Ub system (4). Unlike eukaryotic Ubls, these proteins serve as sulfur carriers in thiamine and molybdopterin synthesis pathways, respectively. Consequently, their mode of action is distinct from that of the canonical *E2–E3* machinery. Instead, both ThiS and MoaD acquire an activated sulfur atom from ThiF/MoeB to yield a thiocarboxylate at their C terminus, and

downstream enzymatic activities are responsible for incorporation of the sulfur into the precursors of the respective enzymatic cofactors (4 and references therein).

Furukawa *et al.* (8) exploited the functional similarities between the prokaryotic and eukaryotic systems by using the *Escherichia coli* ThiS and MoaD as query sequences to search for homologous proteins in *Saccharomyces cerevisiae*. An uncharacterized ORF of 99 aa was identified and designated *URM1* (Ub-related modifier 1). Urm1 is conjugated to yield high-molecular weight, supposedly proteinaceous Urm1 adducts, a process that was termed urmylation. Urmylation depends on Uba4, the putative *E1* enzyme required for Urm1 activation. To our knowledge, other Urm1-directed enzymatic activities have not been reported.

What is the function of this enigmatic modifier? Urm1 deficiency causes pleiotropic phenotypes in *S. cerevisiae*: defects in invasive growth and pseudohyphal development (9), rapamycin sensitivity (10), and derepression of nitrogen catabolite-repressed genes (11) are all suggestive of a promiscuous role in nutrient sensing. In addition, *urm1* Δ strains are temperature-sensitive and hypersensitive toward oxidative stress (8, 10), suggesting a broader role in stress tolerance. The antioxidant protein Ahp1p is the only urmylation target that has been identified to date, and *urm1* Δ strains are hypersensitive toward the oxidant diamide (10). The high degree of sequence conservation suggests an important role for Urm1 in higher eukaryotes as well, but no function has been assigned to it in mammalian cells.

In this work, we investigate the function of Urm1 in human cells. We used a small hairpin RNA (shRNA)-mediated approach to reduce cellular Urm1 levels and observed a strong cytokinesis defect as one of the phenotypic consequences. Furthermore, the application of an Urm1-based suicide inhibitor allowed us to identify ATPBD3, a yet uncharacterized Urm1-dependent enzyme and a constituent of a multiprotein complex. By detecting a cellular Urm1 thiocarboxylate as catalytic intermediate, we show that the underlying mechanism relies on an unexpected sulfur carrier function for Urm1. The activated sulfur is required for the ATPBD3-catalyzed thiolation of certain anticodon nucleosides, as evidenced by the hypomodification of tRNAs in absence of Urm1 or any of the catalytic activities that act on it. We show that this mode of action is operative in *S. cerevisiae* and in human cells, suggesting its strict conservation throughout all eukaryotes.

Author contributions: C.D.S. designed research; C.D.S., A.G.V.d.V., J.R.D., and E.S. performed research; C.D.S., A.G.V.d.V., J.R.D., and E.S. contributed new reagents/analytic tools; C.D.S., A.G.V.d.V., J.R.D., E.S., and H.L.P. analyzed data; and C.D.S., A.G.V.d.V., J.R.D., and H.L.P. wrote the paper

The authors declare no conflict of interest.

This article is a PNAS Direct Submission.

Freely available online through the PNAS open access option.

¹To whom correspondence may be addressed. E-mail: schlieke@wi.mit.edu or ploegh@wi.mit.edu.

This article contains supporting information online at www.pnas.org/cgi/content/full/0808756105/DCSupplemental.

© 2008 by The National Academy of Sciences of the USA

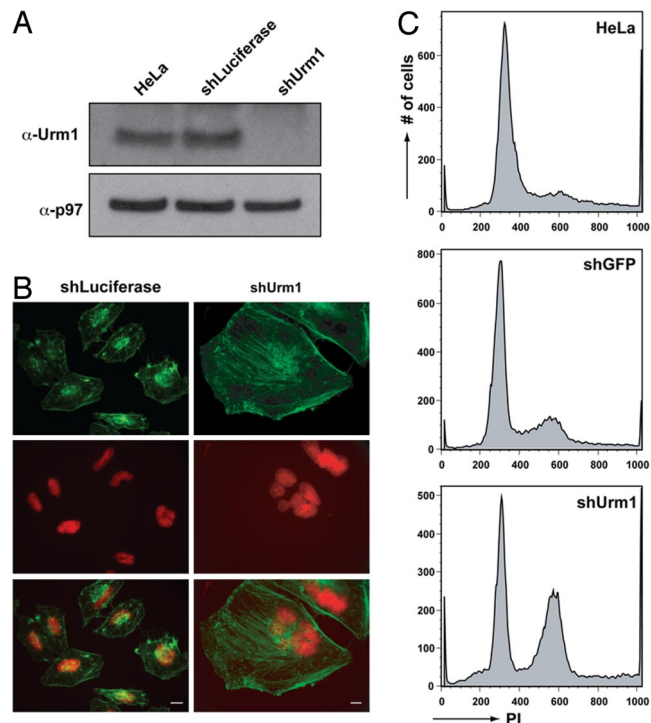


Fig. 1. Depletion of Urm1 results in a cytokinesis defect. (A) Efficiency of Urm1 knockdown in HeLa cells 4 days after lentiviral transduction of luciferase (control) or Urm1 shRNA constructs. (B) Confocal microscopy of Urm1-depleted HeLa cells. Red, Hoechst; green, actin. (Scale bars, 10 μ m.) (C) Progress through cell cycle was assessed by quantification of DNA content in wild-type, shGFP, and shUrm1 HeLa cells. The DNA content of cells was quantified by flow cytometry 12 h after release from a double-thymidine block and plotted in a histogram.

Results

Reduced Urm1 Levels Cause Cytokinesis Defects in Human Cells. To investigate the effects of Urm1 deficiency in mammalian cells, we targeted the Urm1-coding sequencing in HeLa cells with a shRNA by means of lentiviral transduction. We obtained a significant ($\approx 95\%$) and highly reproducible reduction of Urm1 protein levels 4 days after infection (Fig. 1A). The unrelated control shRNA (shLuciferase or shGFP) did not affect Urm1 protein levels (Fig. 1A and data not shown). ShUrm1 cells were viable but showed a reduced growth rate compared with shLuciferase cells. After ≥ 3 days of drug selection, shUrm1 cells exhibited remarkable morphological anomalies: we observed an increase in cell size and the presence of multiple nuclei within single cells (Fig. 1B). In contrast, shLuciferase or mock-infected cells were phenotypically normal (Fig. 1B and data not shown).

To measure the DNA content of these cells, asynchronously growing cells transduced with shUrm1 or shGFP were stained with propidium iodide and analyzed by flow cytometry. Consistent with the multinucleated phenotype, shUrm1 cells showed a significant increase in the $4n$ population, and in addition a population containing $>4n$ was present. The DNA content of shGFP cells was essentially unchanged compared with wild-type HeLa cells. The effects of Urm1 deficiency on DNA content were even more pronounced after cell cycle synchronization by imposition of a double-thymidine block (Fig. 1C). Twelve hours after release from this block, 53.3% of shUrm1 cells contained $\geq 4n$, compared with 31.0% and 31.2% for shGFP and mock-infected cells, respectively. Similar results were observed in asynchronously growing U2OS cells in which Urm1 protein levels were successfully down-regulated (data not shown).

Taken together, our results suggest that Urm1 is required for cytokinesis and thus for orderly cell cycle progression.

A Functional Proteomics Approach Links Urm1 to tRNA Modification.

To gain insights into the molecular mechanism(s) that underlie this remarkable phenotype, we used a functional proteomics approach. We synthesized an electrophilic Urm1-based suicide inhibitor, HA-tagged Urm1 vinyl methylester (HA-Urm1-VME). The analogous Ub/Ubl-based electrophilic probes form a stable thioether linkage to the active site cysteine of Ub/Ubl-directed enzymes (12, 13) and can thus be used to selectively retrieve cognate enzymatic activities from crude cell extracts to allow their identification (14).

HA-Urm1-VME was added to HEK293T cell lysates and incubated at 37 $^{\circ}$ C for 30 min. Covalent HA-Urm1-VME adducts were retrieved by immunoprecipitation and resolved by SDS/PAGE. After silver staining, a prominent band migrating at an apparent molecular mass of ≈ 47 kDa appeared as unique to the HA-Urm1-VME-derived sample (Fig. S2). This material was excised and processed for liquid chromatography–tandem mass spectrometry (LC-MS/MS). A database search revealed ATPBD3 (ATP-binding domain 3, gi 21687159, theoretical molecular mass 36.4 kDa) as the major HA-Urm1-VME-reactive species (33% sequence coverage, Fig. S2). As expected, Urm1 was also identified in this sample (Fig. S2). The function of ATPBD3 is unknown, but it is annotated as a cancer-associated gene and appears to be differentially expressed in breast and prostate cancer (15).

To confirm this interaction, we constructed a FLAG-tagged version of the ATPBD3 cDNA via RT-PCR and expressed the 35 S-labeled protein by a coupled in vitro transcription–translation system. The translation product was incubated in presence or absence of *N*-ethylmaleimide (NEM), and then exposed to HA-Urm1-VME. A band of the expected ATPBD3 molecular mass was readily detectable, and a shift in electrophoretic mobility indicative of covalent modification was observed upon addition of HA-Urm1-VME (Fig. 2A). This modification was sensitive to NEM, suggesting that a cysteine residue in ATPBD3 is the site of modification. We confirmed these findings by transiently transfecting FLAG-ATPBD3 into HEK293T cells followed by detergent lysis and anti-HA immunoprecipitation in the absence or presence of HA-Urm1-VME. Although FLAG-ATPBD3 was barely detectable in the control lane, a prominent FLAG-reactive band was retrieved in the presence of HA-Urm1-VME (Fig. 2B). In addition, a higher-molecular mass doublet is seen in presence of HA-Urm1-VME, which we interpret as the covalent adduct formed between FLAG-ATPBD3 and the suicide inhibitor.

Finally, we used an HA-tagged variant of ATPBD3 to retrieve and identify additional interaction partners. To this end, HEK293T cells were transiently transfected either with a control vector or with ATPBD3-HA. Cell extracts were prepared 48 h after transfection, and ATPBD3-associated proteins were retrieved by immunoprecipitation, separated by SDS/PAGE, and subjected to silver staining. A total of 4 bands appeared to be unique species compared with the negative control (Fig. 2C). These were excised and processed for identification by mass spectrometry (MS). Notably, Urm1 was readily detectable as interaction partner in this experiment (Fig. 2C, sequence coverage 48.5%). As expected, ATPBD3 accounted for the major band, migrating at the expected apparent molecular mass of ≈ 38 kDa. The 2 major species recovered from the other bands correspond to UPF0432 protein/C16orf84, a yet uncharacterized protein (gi 121941955, molecular mass 56 kDa, 36% sequence coverage), and Hsp70 (gi 167466173, molecular mass 70 kDa, 66% sequence coverage), a common contaminant that is encountered in many MS-based approaches.

Because no function was assigned to either human ATPBD3 or UPF0432, we used a structure prediction-based algorithm (16) to search for structural homologues. MesJ [Protein Data Bank (PDB) ID code 1ni5], an ATP α -hydrolase of unknown function, and TilS (PDB ID code 1wy5), a tRNA-modifying enzyme and likewise an ATP α -hydrolase, were predicted as closest structural neighbors for both ATPBD3 and UPF0432 (data not shown). A Pfam search (17) consistently assigned both proteins to the PP-loop ATP pyro-

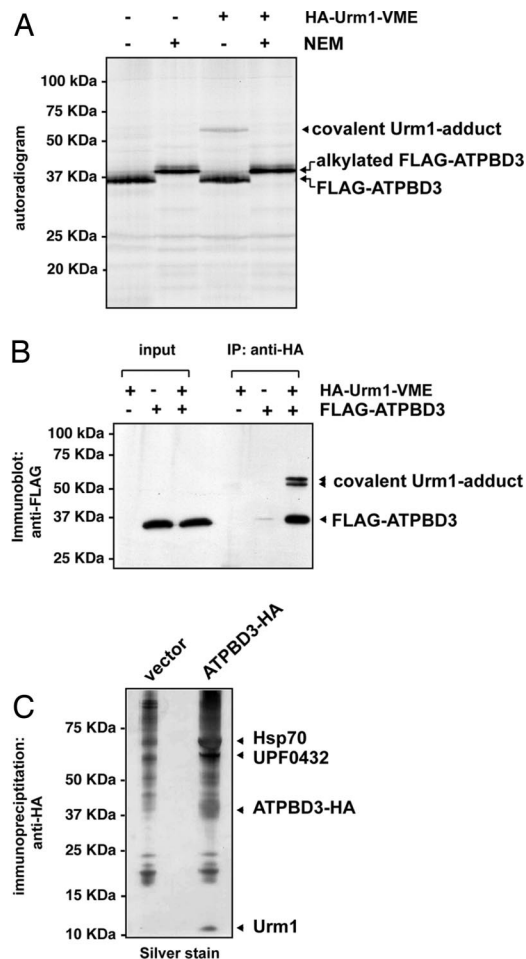


Fig. 2. A Urm1-based functional probe reacts with ATPBD3, a Urm1-directed enzymatic activity. (A) HA-Urm1-VME reacts with ATPBD3 to yield a covalent adduct. Radiolabeled ATPBD3 was synthesized by *in vitro* translation, reacted with HA-Urm1-VME in the absence or presence of NEM, and resolved by SDS/PAGE. (B) HA-Urm1-VME retrieves ATPBD3 from cell lysates. HEK293T cells were transfected with FLAG-ATPBD3 or control vector (–), lysed, exposed to HA-Urm1-VME, and immunoprecipitated (IP) with anti-HA antibodies. Anti-FLAG antibodies were used for detection. (C) Overexpressed ATPBD3 associates with endogenous UPF0432 and Urm1 *in vivo*. HEK293T cells were transfected with ATPBD3-HA, lysed, and immunoprecipitated with anti-HA antibodies. After SDS/PAGE and silver staining, the indicated ATPBD3-associated proteins were identified by MS.

phosphatase family, which comprises a plethora of tRNA-modifying enzymes. From a structural perspective, these findings collectively suggest a link between Urm1 and tRNA modifications. Genetic evidence likewise suggests that the budding yeast homologs of UPF0432 and ATPBD3, *NCS2* and *NCS6*, respectively, are linked to the Urm1 pathway: *NCS2* (needs *Cla4* to survive) and *NCS6* deletions are both synthetic lethal in the absence of *Cla4*, a protein kinase involved in septin phosphorylation. This phenotype is mirrored by *Uba4* and *Urm1* deletions, which are essential when *Cla4* is absent (9). More recently, the fission yeast homologs of UPF0432 and ATPBD3 were designated *Ctu2* and *Ctu1* (cytosolic thiouridylase), respectively. They were shown to form a heterodimeric complex, required for the thiolation of the uridine at the first anticodon position of cytosolic tRNAs (18, 19).

Urm1 Can Serve as Sulfur Carrier by Virtue of a C-Terminal Thiocarboxylate. What could be the function of Urm1 in the context of tRNA modifications? Given the involvement of *Ncs6* (*Ctu1*) in tRNA thiolation and based on the structural similarity between

Urm1 and *MoaD*, we speculate that Urm1 could serve as sulfur carrier in the context of tRNA thiolation in mammalian cells. To test this possibility, HEK293T cells were cotransfected with MOCS3-HA (the human *Uba4* homolog) and HA-Urm1. Soluble cell extracts were prepared 48 h after transfection, HA-Urm1 was retrieved by immunoprecipitation, further purified by SDS/PAGE (Fig. 3A), and digested with the endoprotease Asp-N to yield peptides of a size suitable for analysis by LC-MS/MS. Database searches of the resulting MS data revealed 2 overlapping peptides from the C terminus, indicating that either the Asp-88 or Asp-90 cleavage sites were used (Fig. 3B). In addition, database searching also identified 2 peptides with a mass 16 Da greater than these, with the additional mass localized at the C terminus (Fig. 3B), as shown by the masses of the y ion series (Fig. 3C). This shift in mass is consistent with a C-terminal modification by sulfur in the form of a thiocarboxylate. We conclude that Urm1 can serve as sulfur carrier, akin to the prokaryotic sulfur donors *ThiS* and *MoaD*.

Cytosolic tRNAs Are Hypomodified in the Absence of Urm1. In *S. cerevisiae*, 3 cytosolic tRNAs, tRNA^{Gln(UUG)}, tRNA^{Glu(UUC)}, and tRNA^{Lys(UUU)} contain a 5-methylcarboxymethyl-2-thiouridine (*mcm*⁵S²U) at the wobble position (19) (Fig. 4A). Several enzymatic activities act on the 2- and 5-positions of the uridine ring in yeast: *Elp3* has been implicated in the derivatization of the 5-position (20), and *Ctu1/NCS6* is required for the 2-thiolation (19). However, the source of the sulfur atom that is used by *Ctu1/NCS6* remains enigmatic. With the exception of *Mycoplasma*, 2-thiolated uridines have been identified in all kingdoms of life. Notably, the simultaneous loss of *Elp3* and *Ctu1* is lethal, indicating a crucial role for these modifications (19).

Can Urm1 serve as sulfur donor for the *Ctu1/Ncs6*-catalyzed thiolation reaction? Because the enzymatic pathway responsible for uridine modification is well characterized in yeast, we chose to address this question by introducing chromosomal deletions in *S. cerevisiae*. Four deletion strains were constructed: *urm1Δ*, *uba4Δ*, *nsc6Δ*, and *cla4Δ*. To assess the extent of tRNA^{Gln(UUG)}, tRNA^{Glu(UUC)}, and tRNA^{Lys(UUU)} thiolation, RNA was isolated from all deletion strains; a wild-type (WT) strain served as control (Fig. 4B). The RNA was separated on a denaturing polyacrylamide gel supplemented with *N*-acryloylamino phenyl mercuric (APM) chloride and transferred to a nylon membrane. Small radiolabeled DNA oligonucleotides complementary to the 3 tRNAs in question were used as probes; a probe recognizing the nonthiolated tRNA^{His} served as negative control. The thiolation of RNA molecules is readily detectable in APM gels by transient mercury–sulfur interactions, which cause a considerable shift in electrophoretic mobility (21). In agreement with the established role of *Ncs2/Ctu1* in 2-thiolation (19), the deletion of *NCS6* caused an increase in tRNA^{Lys(UUU)} mobility, indicative of quantitative hypomodification. RNA isolates from *cla4Δ* behaved like the WT control, suggesting that *Cla4* is not directly involved in this process (Fig. 4B). Remarkably, the *Urm1* deletion mirrored the effect seen in a *nsc6Δ* background, indicative of a quantitative loss of thiolation (Fig. 4B). Virtually identical results were obtained for tRNA^{Gln(UUG)} and tRNA^{Glu(UUC)} (Fig. S3). As an additional control, the RNA samples were applied to denaturing PAGE devoid of APM: all samples showed an identical electrophoretic behavior (Fig. S3), thus excluding the formal possibility that a difference in length is responsible for the differential migration behavior as seen in Fig. 4B.

To substantiate our findings, we hydrolyzed RNA isolated from WT and *urm1Δ* strains for analysis by LC-MS. For the WT control, we observed masses corresponding to 5-methylcarboxymethyluridine (*mcm*⁵U) and *mcm*⁵S²U. We did not detect *mcm*⁵S²U in *urm1Δ*-derived hydrolysates, whereas *mcm*⁵U was clearly detectable (Fig. S4). We conclude that Urm1 is required for the thiolation of 3 cytosolic tRNA species, namely tRNA^{Gln(UUG)}, tRNA^{Glu(UUC)}, and tRNA^{Lys(UUU)}.

To establish that tRNA thiolation is Urm1-dependent in higher

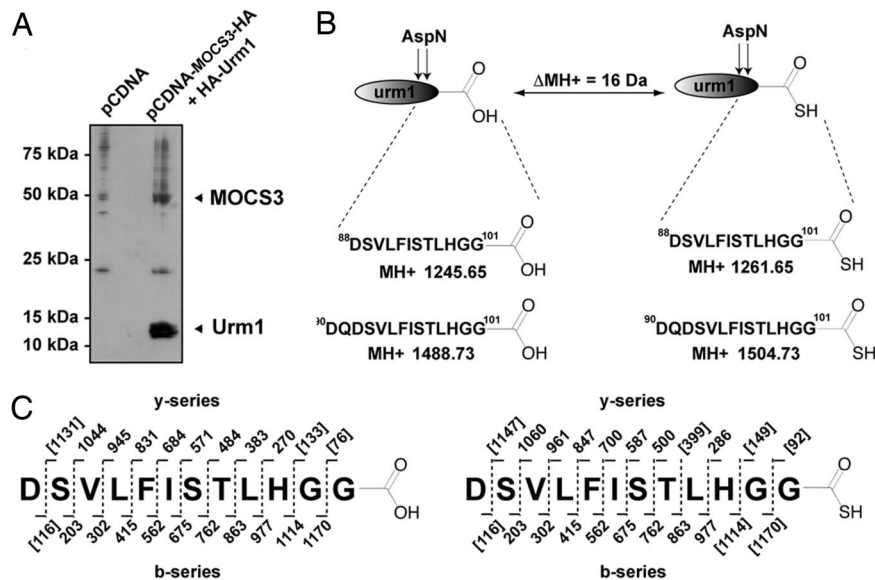


Fig. 3. Urm1 is charged with sulfur in vivo to form of a C-terminal thiocarboxylate. (A) HEK293T cells were cotransfected with MOCs3-HA and HA-Urm1, lysed, and subjected to immunoprecipitation with anti-HA antibodies. The immunoprecipitates were resolved by SDS/PAGE and subjected to silver staining. Note that both proteins were HA-tagged, i.e., the appearance of MOCs3-HA and HA-Urm1 is not indicative of a mutual interaction. (B) The band marked in A was excised, digested with Asp-N, and analyzed by LC-MS/MS. The observed parent ion masses are consistent with Asp-N-released peptides from the C terminus of Urm1 and suggest that both unmodified and thiocarboxylated Urm1 were present (the mass difference between sulfur and oxygen is 16 Da). (C) Note that the y-ion series (i.e., the series containing the C terminus), derived from fragmentation of the smaller parent ions depicted in B, is in excellent agreement with the location of the sulfur at the C terminus. Masses in brackets are theoretical and were not observed in this experiment.

eukaryotes, we reduced the levels of Urm1 and ATPBD3 via lentivirus-transduced shRNA in HeLa cells. Total RNA was extracted from the resulting HeLa cell lines propagated under selective pressure for 3 days. Because appropriate antisera were not available for ATPBD3, we cannot assess the knockdown efficacy achieved by the respective shRNA. However, an accumulation of hypomodified cytosolic tRNA^{Lys(UUU)} was seen in all cell lines relative to the shGFP control, as judged by APM-PAGE/Northern blot analysis (Fig. 4 C and D). Taken together, the levels of thiolated tRNAs are correlated to cellular Urm1-levels in 2 distinct organisms, indicating that the role for Urm1 in these pathways is evolutionarily conserved.

Discussion

Urm1 is a highly conserved, yet poorly understood, ubiquitin-related modifier. Urm1-deficient yeast strains show a pleiotropic

phenotype, attributed to a lack of Urm1 conjugation to target proteins, a process that was termed urmylation (8–11). Apart from the identity of Uba4, the putative E1 enzyme responsible for Urm1 activation (8), next to nothing is known about the molecular mechanism and the enzymatic machinery that constitute the Urm1 pathway.

By using an Urm1-based suicide inhibitor, we discovered ATPBD3 as an Urm1-directed enzymatic activity (Fig. S2 and Fig. 2). Urm1 is part of a protein complex that contains ATPBD3 and UPF0432 (Fig. 2C and data not shown). However, neither of these proteins has been assigned a function. A bioinformatics approach revealed similarities of both ATPBD3 and UPF0432 to tRNA-modifying enzymes, which commonly adenylate specific tRNA nucleosides to facilitate their subsequent derivatization. What could be the function of Urm1 in the context of tRNA modifications?

The *S. cerevisiae* homolog of ATPBD3, Ncs6, is required for the thiolation of uracil at the wobble position of U-rich anticodons of

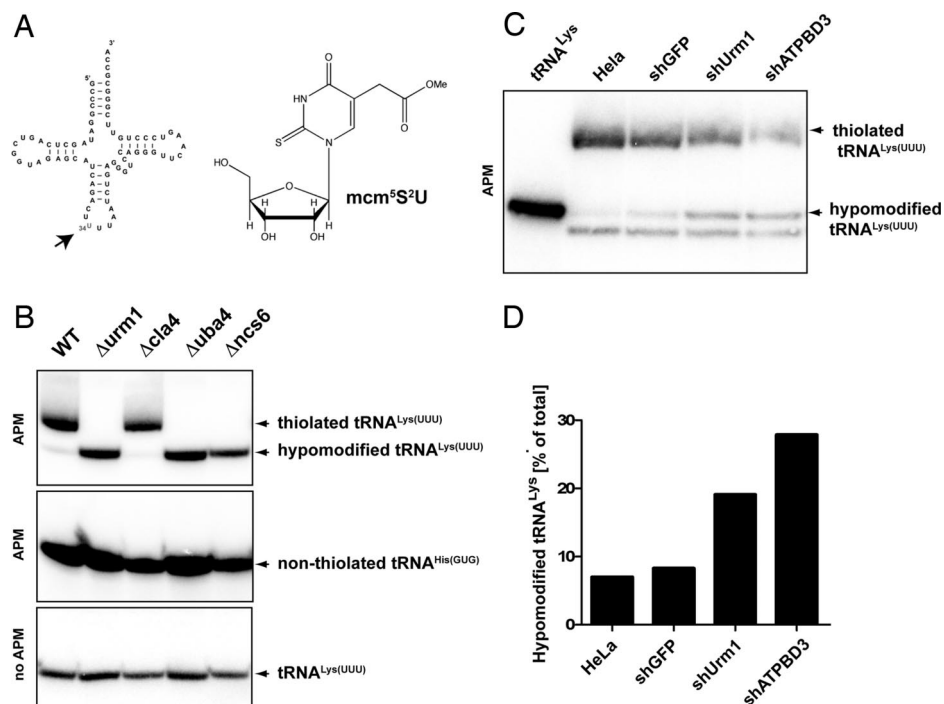


Fig. 4. Urm1 is required for the thiolation of cytosolic tRNAs. (A) U-rich anticodons of several cytosolic tRNAs, exemplified by the human tRNA^{Lys(UUU)}, contain a modified uracil, mcm⁵S²U, at position 34. (B) Urm1 and Urm1-associated enzymatic activities are required for tRNA thiolation in *S. cerevisiae*. RNA was isolated from the indicated *S. cerevisiae* strains, resolved by denaturing PAGE, and subjected to Northern blotting. Polyacrylamide gels supplemented with APM served as control (Bottom). The indicated nonthiolated tRNA^{His} serves as control (Middle). Radioactive oligonucleotides with the indicated specificities served as probes. (C) Urm1 and ATPBD3 contribute to tRNA thiolation in human cells. RNA isolated from the indicated HeLa cell lines was analyzed as in B, purified unmodified tRNA^{Lys(UUU)} (5 pmol) served as control. (D) Comparison of thiolation levels obtained from a densitometric quantification of the bands seen in C.

3 cytosolic tRNAs (19). Moreover, a protein complex homologous to ATPBD3-UPF0432, Ctu1-Ctu2, was recently identified in *Schizosaccharomyces pombe* and likewise implicated in uracil thiolation (18). Genetic evidence suggests that *URM1*, *NCS2* (the UPF0432 homolog), and *NCS6* are linked in budding yeast (9, 22), but the functional connection between *Ncs2*, *Ncs6* and *Urm1* remained unclear.

Urm1 is in fact more similar to the prokaryotic sulfur carriers *MoaD* and *ThiS* than it is to any bona fide Ub-like protein modifier (Fig. S1). Moreover, *Uba4* and *MOCS3*, the human *Uba4* homolog, are more similar to the *MoaD*-activating enzyme *MoeB* than to the *E1* enzymes that participate in the typical *E1-E2-E3* cascades. *Uba4/MOCS3* both feature a rhodanese-like domain, a module that is commonly involved in sulfur transfer. Although purified *Uba4* displays sulfur transfer activity in vitro, it was unclear whether this activity is relevant in a cellular context (23). All in all, these criteria suggest that the *Urm1* pathway is mechanistically closely related to the prokaryotic *MoaD* and *ThiS* pathways (1, and references cited therein; 4, 24). Specifically, we propose that *Urm1* serves as sulfur donor in the context of tRNA thiolation.

We isolated HA-*Urm1* introduced into mammalian cells by transfection and showed that peptides derived from the *Urm1* C terminus were present as 2 species, corresponding to unmodified *Urm1* and to a C-terminal thiocarboxylate (Fig. 3 B and C). This observation supports our hypothesis and is an example of a Ub-related modifier that undergoes a thiocarboxylation reaction in human cells. Furthermore, we show that the deletion of *URM1*, *UBA4*, or *NCS6* results in a quantitative loss of thiolation of 3 cytosolic tRNAs in *S. cerevisiae* (Fig. 4B). Consistently, the mcm^5S^2U fingerprint mass was not detectable in nucleoside preparations isolated from *urm1Δ* strains (Fig. S4). In human cells, a reduction in the levels of either *Urm1* or ATPBD3 likewise resulted in an increase of hypomodified tRNAs^{LYS(UUU)} (Fig. 4D), suggesting a similar, if not identical, function for *Urm1* in both organisms. Although UPF0432 associates with ATPBD3, we did not observe covalent adduct formation between *Urm1*-VME and UPF0432 (data not shown). We speculate that UPF0432 might be involved in the *Urm1*-independent derivatization of the 5-position. The failure to obtain complete suppression of thiolation by *Urm1* knockdowns in mammalian cells could indicate that residual *Urm1* levels are adequate to sustain the observed tRNA thiolation levels. Based on these results, we assign a conserved sulfur carrier function to *Urm1*.

How the sulfur is mobilized upstream of *Uba4/MOCS3* is not known. The cysteine desulfurase *Nsf1*, a pyridoxal 5' phosphate (PLP)-dependent enzyme implicated in tRNA thiolation (25), binds to the RLD domain of *MOCS3*, where it can generate a persulfidic intermediate in vitro (26). In this scenario, the sulfur flux would start by a *Nsf1*-catalyzed sulfur transfer from L-cysteine to *MOCS3*, and *MOCS3* would use the sulfur to charge *Urm1* to yield a thiocarboxylate. Finally, ATPBD3 would transfer the sulfur from the *Urm1* thiocarboxylate to the 2-position of uracil, a suggestion that can only be confirmed by detailed structural analysis.

While this manuscript was in preparation, Nakai *et al.* (27) placed *Urm1* in the tRNA thiolation pathway in *S. cerevisiae* and arrived at similar conclusions, although evidence for thiocarboxylate formation on *Urm1* was not presented. Consistent with this report and our study, deletions in any of the components that now define the *Urm1* pathway (*MOCS3*, *Urm1*, ATPBD3 in humans; *Uba4*, *Urm1*, *Ncs6* in budding yeast), or those that are required for the derivatization of the 5-position of the uridine, confer resistance to the *Kluyveromyces lactis* killer toxin (20, 22, 28, 29). This toxin exerts its effect by cleaving the anticodon loop of tRNAs, and the presence of uridine modifications is a prerequisite for the killer toxin's nuclease activity (30).

As far as the pleiotropic consequences of *Urm1* mutations under stress conditions are concerned, many mutations in the *Urm1* pathway should affect the modification of at least 3 tRNA species. Because 2-thio modifications have been implicated in translational

fidelity and efficacy (31–33), translational errors and ultimately protein misfolding are the unavoidable outcomes when thiolation is suppressed. As a consequence, the respective mutant strains will display an increased sensitivity against multiple stress conditions, irrespective of a specific function of *Urm1* in a given stress response pathway.

How can the sulfur carrier function of *Urm1* be linked to the observed cytokinesis defect (Fig. 1)? A similar phenotype was observed in 14-3-3σ knockdown cells, where it was attributed to a defect in translation control at the G₂/M transition (34). Dewez *et al.* (18) reported aneuploidy as a phenotypic consequence of the *Ctu1* deletion, and mislocalized septa were reported in the context of mutations in the *Urm1* pathway in budding and fission yeast (9). Along the same line, inosine modifications have been implicated in G₁/S and G₂/M transitions in fission yeast (35). We did not observe obvious changes of tRNA thiolation as a function of the cell cycle, neither in synchronized HeLa cells nor in synchronized *S. cerevisiae* cultures, thus excluding dynamic fluctuations in this modification as key regulatory mechanism (data not shown). One interpretation would be that the cytokinesis defect is a mere consequence of cellular senescence, which is in turn promoted by translational defects. Alternatively, some of the transcripts that encode key regulators of the cell cycle may be particularly enriched in codons that are read by 2-thiolated tRNAs. Interestingly, skewed codon usage patterns occur in functionally related genes, or groups, and have been linked to tRNA modifications (36 and references cited therein).

The sulfur donor function identified here is not necessarily restricted to tRNAs. The involvement of *Urm1* in protein conjugation and a role in tRNA thiolation are not mutually exclusive, and further experiments are required to identify or to rule out additional *Urm1* functions.

Experimental Procedures

Cell Lines, Antibodies, Constructs, and Lentiviral Transduction. *Cells.* HeLa cells were cultured in DMEM containing 10% fetal calf serum and penicillin/streptomycin at 37 °C, 5% CO₂.

Antibodies. Human *Urm1* was expressed as N-terminal His-tagged fusion protein in *E. coli* BL21 (DE3) Rosetta cells, purified, and sent to Covance Research Products to generate rabbit polyclonal antibodies. The antiserum was affinity-purified as described in ref. 37. Anti-p97 was purchased from Fitzgerald Industries International. Anti-FLAG and anti-HA (3F10) were purchased from Sigma and Roche, respectively. Phalloidin-647 and Hoechst 33342 were from Molecular Probes.

Constructs. Human cDNA was prepared from HeLa cells with the SuperScript first-strand synthesis system (Invitrogen) and used as template for PCRs to amplify the human *Urm1*, *MOCS3*, and ATPBD3 cDNAs. All constructs were cloned into pcDNA3.1⁺ (Invitrogen) according to standard procedures.

Lentivirus. Human *Urm1*, ATPBD3 and control (GFP and luciferase) shRNA constructs were obtained from the TRC Consortium at the Broad Institute of MIT and Harvard (Boston, MA). Lentivirus was produced according to instructions provided by the Broad Institute (www.broad.mit.edu/genome.bio/trc/publicProtocols.html). HeLa cells were infected in a 6-well plate with 100–500 μL of viral supernatant supplemented with 4 μg/mL Polybrene (Sigma), spun at 1,020 × g for 90 min at room temperature and placed for 5 h in the incubator before medium replacement. Antibiotic selection (1 μg/mL puromycin) was started 24 h after infection.

Transfections. All transfections were carried out by using Lipofectamine 2000 (Invitrogen), according to the manufacturer's instructions.

Confocal Microscopy. Cells were grown on coverslips, fixed in 4% paraformaldehyde, quenched with 20 mM glycerine, 50 mM NH₄Cl, and permeabilized in 0.1% Triton X-100. Fixed and permeabilized cells were blocked in 4% BSA and stained with phalloidin-647 and Hoechst for 30 min. Images were acquired by using a spinning disk confocal microscope as described in ref. 38 by using a Nikon 60× magnification, 1.4 numerical aperture oil lens.

Flow Cytometry. Cell synchronization by double-thymidine block was performed as described in ref. 34. Cells were harvested by trypsinization at 12 h after release from cell cycle block, fixed in ice-cold 70% ethanol, and stained with propidium iodide (50 μg/mL) in the presence of 0.1 mg/mL RNase A and 0.05% Triton X-100 for 40 min at 37 °C. Cells were analyzed by using a Becton Dickinson FACSCalibur, and cell cycle profiles were generated by using FlowJo 8.5.3 software.

Anti-HA Affinity Purification and MS/MS Analysis. HA-Urm-VME was produced as described for Ub-VME (39). HEK293T cells (10^8) were harvested by scraping in ice-cold PBS and centrifugation. The pellet was resuspended in 10 mL of lysis buffer (50 mM Tris, 150 mM NaCl, 5 mM MgCl₂, 0.5% Nonidet P-40, 0.5 mM DTT, pH 7.5) and incubated on ice for 10 min. The lysate was clarified by centrifugation ($14,000 \times g$ for 15 min at 4 °C). The supernatant was incubated in presence (or absence) of 50 μ g of HA-Urm-VME for 30 min at 37 °C, supplemented with anti-HA-agarose (80 μ L of slurry 3F10 affinity beads; Roche), and agitated for 2 h at 4 °C. The beads were washed 4 times in wash buffer (50 mM Tris, 150 mM NaCl, 5 mM MgCl₂, 0.1% Nonidet P-40), eluted by boiling in 60 μ L of SDS-sample buffer and applied to a SDS/PAGE and silver staining. For protein identification, bands were excised, processed, and analyzed by LC-MS/MS as described in ref. 37. For thiocarbonylate detection, samples were digested with endoproteinase Asp-N instead of trypsin.

For immunoprecipitations, one 10-cm dish of subconfluent HEK293T cells was harvested 48 h after transfection and solubilized in 1 mL of ice-cold lysis buffer supplemented with Complete (Roche) and centrifuged ($14,000 \times g$ for 10 min at 4 °C). Sixteen microliters of 3F10 beads were added to the supernatant and agitated for 3–4 h at 4 °C, washed 3 times in wash buffer, and eluted by boiling in 30 μ L of SDS-sample buffer. Five micrograms of HA-Urm1-VME was added to 1 mL of clarified lysate for small-scale reactions and reacted for 30 min at 37 °C before immunoprecipitation.

In Vitro Transcription/Translation (IVT). IVT reactions were performed by using the TNT system (Promega), according to the manufacturer's instructions. Five micrograms of HA-Urm1-VME was applied to 50 μ L of IVT reaction and incubated for 30 min at 30 °C before loading on a gel. A final concentration of 10 mM NEM was applied to the indicated samples before addition of HA-Urm-VME.

Yeast Techniques and RNA Analysis. Yeast strains. All strains are W303 derivatives and are described in Table 1. Gene deletions were constructed by using the method described (40) to replace the desired ORF with either the *HIS3MX6* or the *KANMX6* cassette. All deletions were confirmed by PCR. *cla4 Δ* was a

Table 1. Yeast strains and genotypes used in this work

Strain	Relevant genotype
8015 (wild-type) (from A. Amon)	MATa
<i>urm1Δ</i>	MATa <i>urm1Δ::KANMX6</i>
<i>ncs6Δ</i>	MATa <i>ncs6Δ::HIS3MX6</i>
<i>uba4Δ</i>	MATa <i>uba4Δ::HIS3MX6</i>
<i>cla4Δ</i> (from A. Amon)	MATa <i>cla4Δ::HIS3MX6</i>

kind gift from the laboratory of Angelika Amon (Massachusetts Institute of Technology, Cambridge, MA).

RNA MS analysis. For MS analysis of yeast tRNA, yeast cultures were grown at 30 °C and harvested in mid log phase. RNA was prepared by using the Qiagen RNA/DNA kit (Qiagen14162) and processed for MS analysis as described (41, 42).

Northern Blot Analysis. RNA for analysis by Northern blotting was prepared by using TRIzol reagent (Invitrogen) to isolate total RNA according to the manufacturer's instructions. Ten micrograms of RNA (isolated from yeast or HeLa cells) was run on either 8% PAGE gels (Sequagel; National Diagnostics) or on APM gels (8% PAGE gels with addition of 20 μ M APM). Gels were transferred to GeneScreen Plus membrane (PerkinElmer), UV-cross-linked, and processed according to standard procedures. DNA probes complementary to the tRNA sequences (either mammalian or yeast) of Lys-tK(UUU), Glu-tE(UUC) or Gln-tQ(UUG) were end-labeled with [γ -³²P]ATP (PerkinElmer) by using T4 polynucleotide kinase (NEB).

ACKNOWLEDGMENTS. We thank Uttam Rajbhandary, Thomas Carlile, and Calvin Jan for helpful discussions; the laboratory of Angelika Amon for strains; and Nicholas Yoder for help with the APM synthesis. C.D.S. was supported by European Molecular Biology Organization Long-Term Fellowship 187-2005. A.G.V.d.V. was supported by the Boehringer Ingelheim Fonds.

- Kerscher O, Felberbaum R, Hochstrasser M (2006) Modification of proteins by ubiquitin and ubiquitin-like proteins. *Annu Rev Cell Dev Biol* 22:159–180.
- Capili AD, Lima CD (2007) Taking it step by step: Mechanistic insights from structural studies of ubiquitin/ubiquitin-like protein modification pathways. *Curr Opin Struct Biol* 17:726–735.
- Dye BT, Schulman BA (2007) Structural mechanisms underlying posttranslational modification by ubiquitin-like proteins. *Annu Rev Biophys Biomol Struct* 36:131–150.
- Iyer LM, Burroughs AM, Aravind L (2006) The prokaryotic antecedents of the ubiquitin-signaling system and the early evolution of ubiquitin-like β -grasp domains. *Genome Biol* 7:R60.
- Daniels JN, Wuebbens MM, Rajagopalan KV, Schindelin H (2008) Crystal structure of a molybdopterin synthase-precursor Z complex: Insight into its sulfur transfer mechanism and its role in molybdenum cofactor deficiency. *Biochemistry* 47:615–626.
- Duda DM, Walden H, Sfendouris J, Schulman BA (2005) Structural analysis of *Escherichia coli* ThiF. *J Mol Biol* 349:774–786.
- Lehmann C, Begley TP, Ealick SE (2006) Structure of the *Escherichia coli* ThiS–ThiF complex, a key component of the sulfur transfer system in thiamin biosynthesis. *Biochemistry* 45:11–19.
- Furukawa K, Mizushima N, Noda T, Ohsumi Y (2000) A protein conjugation system in yeast with homology to biosynthetic enzyme reaction of prokaryotes. *J Biol Chem* 275:7462–7465.
- Goehring AS, Rivers DM, Sprague GF, Jr (2003) Urm1ylation: A ubiquitin-like pathway that functions during invasive growth and budding in yeast. *Mol Biol Cell* 14:4329–4341.
- Goehring AS, Rivers DM, Sprague GF, Jr (2003) Attachment of the ubiquitin-related protein Urm1p to the antioxidant protein Ahp1p. *Eukaryot Cell* 2:930–936.
- Rubio-Texeira M (2007) Urm1ylation controls Nil1p and Gln3p-dependent expression of nitrogen-catabolite repressed genes in *Saccharomyces cerevisiae*. *FEBS Lett* 581:541–550.
- Misaghi S, et al. (2005) Structure of the ubiquitin hydrolase UCH-L3 complexed with a suicide substrate. *J Biol Chem* 280:1512–1520.
- Schlieker C, et al. (2007) Structure of a herpesvirus-encoded cysteine protease reveals a unique class of deubiquitinating enzymes. *Mol Cell* 25:677–687.
- Borodovsky A, et al. (2002) Chemistry-based functional proteomics reveals novel members of the deubiquitinating enzyme family. *Chem Biol* 9:1149–1159.
- Yousef GM, et al. (2004) Molecular cloning of a new gene which is differentially expressed in breast and prostate cancers. *Tumour Biol* 25:122–133.
- McGuffin LJ, Bryson K, Jones DT (2000) The PSIPRED protein structure prediction server. *Bioinformatics* 16:404–405.
- Finn RD, et al. (2008) The Pfam protein families database. *Nucleic Acids Res* 36:D281–D288.
- Dewez M, et al. (2008) The conserved wobble uridine tRNA thiolase Ctu1–Ctu2 is required to maintain genome integrity. *Proc Natl Acad Sci USA* 105:5459–5464.
- Bjork GR, Huang B, Persson OP, Bystrom AS (2007) A conserved modified wobble nucleoside (mcm5s2U) in lysyl-tRNA is required for viability in yeast. *RNA* 13:1245–1255.
- Huang B, Johansson MJ, Bystrom AS (2005) An early step in wobble uridine tRNA modification requires the elongator complex. *RNA* 11:424–436.
- Igloi GL (1988) Interaction of tRNAs and of phosphorothioate-substituted nucleic acids with an organomercurial: Probing the chemical environment of thiolated residues by affinity electrophoresis. *Biochemistry* 27:3842–3849.
- Fichtner L, et al. (2003) Elongator's toxin-target (TOT) function is nuclear localization sequence-dependent and suppressed by post-translational modification. *Mol Microbiol* 49:1297–1307.
- Schmitz J, et al. (2008) The sulfurtransferase activity of Uba4 presents a link between ubiquitin-like protein conjugation and activation of sulfur carrier proteins. *Biochemistry* 47:6479–6489.
- Xu J, et al. (2006) Solution structure of Urm1 and its implications for the origin of protein modifiers. *Proc Natl Acad Sci USA* 103:11625–11630.
- Nakai Y, et al. (2004) Yeast Nfs1p is involved in thio-modification of both mitochondrial and cytoplasmic tRNAs. *J Biol Chem* 279:12363–12368.
- Marelja Z, Stocklein W, Nimtz M, Leimkuhler S (2008) A novel role for human Nfs1 in the cytoplasm: Nfs1 acts as a sulfur donor for MOCS3, a protein involved in molybdenum cofactor biosynthesis. *J Biol Chem* 283:25178–25185.
- Nakai Y, Nakai M, Hayashi H (2008) Thio modification of yeast cytosolic tRNA requires a ubiquitin-related system that resembles bacterial sulfur transfer systems. *J Biol Chem* 283:27469–27476.
- Lu J, Huang B, Esberg A, Johansson MJ, Bystrom AS (2005) The *Kluyveromyces lactis* γ -toxin targets tRNA anticodons. *RNA* 11:1648–1654.
- Huang B, Lu J, Bystrom AS (2008) A genomewide screen identifies genes required for formation of the wobble nucleoside 5-methoxycarbonylmethyl-2-thiouridine in *Saccharomyces cerevisiae*. *RNA* 14:2183–2194.
- Lu J, Esberg A, Huang B, Bystrom AS (2008) *Kluyveromyces lactis* γ -toxin, a ribonuclease that recognizes the anticodon stem-loop of tRNA. *Nucleic Acids Res* 36:1072–1080.
- Ikeuchi Y, Shigi N, Kato J, Nishimura A, Suzuki T (2006) Mechanistic insights into sulfur relay by multiple sulfur mediators involved in thiouridine biosynthesis at tRNA wobble positions. *Mol Cell* 21:97–108.
- Kruger MK, Pedersen S, Hagerwall TG, Sorensen MA (1998) The modification of the wobble base of tRNA^{Glu} modulates the translation rate of glutamic acid codons in vivo. *J Mol Biol* 284:621–631.
- Yarian C, et al. (2002) Accurate translation of the genetic code depends on tRNA modified nucleosides. *J Biol Chem* 277:16391–16395.
- Wilker EW, et al. (2007) 14-3-3 σ controls mitotic translation to facilitate cytokinesis. *Nature* 446:329–332.
- Tsutsumi S, et al. (2007) Wobble inosine tRNA modification is essential to cell cycle progression in G₁/S and G₂/M transitions in fission yeast. *J Biol Chem* 282:33459–33465.
- Begley U, et al. (2007) Trm9-catalyzed tRNA modifications link translation to the DNA damage response. *Mol Cell* 28:860–870.
- Lilley BN, Ploegh HL (2004) A membrane protein required for dislocation of misfolded proteins from the ER. *Nature* 429:834–840.
- Vyas JM, et al. (2007) Tubulation of class II MHC compartments is microtubule dependent and involves multiple endolysosomal membrane proteins in primary dendritic cells. *J Immunol* 178:7199–7210.
- Borodovsky A, et al. (2005) Small-molecule inhibitors and probes for ubiquitin- and ubiquitin-like-specific proteases. *Chembiochem* 6:287–291.
- Longtine MS, et al. (1998) Additional modules for versatile and economical PCR-based gene deletion and modification in *Saccharomyces cerevisiae*. *Yeast* 14:953–961.
- Crain PF (1990) Preparation and enzymatic hydrolysis of DNA and RNA for mass spectrometry. *Methods Enzymol* 193:782–790.
- Pomerantz SC, McCloskey JA (1990) Analysis of RNA hydrolysates by liquid chromatography–mass spectrometry. *Methods Enzymol* 193:796–824.